# NUMERICAL ANALYSIS OF SMALL-SCALE CONCRETE BEAMS STRENGTHENED WITH CFRP UNDER IMPACT LOADING

Darya MEMON[1], Stijn MATTHYS[1], David LECOMPTE[2]

1. Magnel-Vandepitte Laboratory for Concrete Research, Department of Structural Engineering and Building Materials, Faculty of Engineering and Architecture, Ghent University, Belgium.
2. Protective and Military Engineering Department, Royal Military Academy of Brussels, Belgium.

Corresponding author email: darya.memon@ugent.be

## Abstract

Reinforced concrete structures are vulnerable to impact loads (e.g. rock-fall, vehicle collision or ship impact) during their service life. It is of interest to understand the impact load behaviour of reinforced concrete and its potentially catastrophic failure. This paper presents a preliminary study, on small-scale reinforced concrete beams strengthened with carbon fibre reinforced polymer (CFRP) under low-velocity impact. This study comprises both experimental work, making use of a drop-weight set-up, and a non-linear finite element model (FEM). The FEM was validated using the results achieved from the experiments. On overall, the simulation yielded promising results in a consistent prediction of the displacement and failure behaviour mechanism, though further sensitivity analysis is needed with respect to the modelling of the specimen boundary conditions. In line with observations in literature, the CFRP strengthening of the test specimens demonstrated to be an effective technique to improve the resistance of the reinforced concrete beams under impact load.

*Keywords: Reinforced concrete, impact load, finite element modelling, CFRP strengthening*

## 1. Introduction

Concrete is one of the most frequently used materials for building structures. Generally, concrete is designed to withstand conventional quasi-static loading, however, recent events occurring all over the world have indicated that concrete is vulnerable to impact loads, such as explosions or direct impact by an object. The impact forces could disturb the structural equilibrium which could put structures at risk of collapse, especially in the case of impact sensitive buildings/installations. Impact load scenarios can be considered in the design of new buildings or structures by introducing sufficient residual strength (rather or not in combination with alternative load paths), like in the design of dams, landslide protection structures and nuclear power plants. For existing structures, strengthening with fibre reinforced polymer (FRP) is a possible technique to enhance the impact resistance [1-6]. Externally bonded FRP strips are extensively used for strengthening purposes due to their versatile properties and applicability to any surface with the help of an adhesive [7]. Reinforced concrete members strengthened with FRP tested under static loads have been thoroughly examined in the past and resulted in mainstream design recommendations such as ACI 440.2R-17 [8] and *fib* Bulletin-90 [9]. Externally bonded FRP reinforcement has also shown promising applicability for reinforced concrete under impact loading, though discussed in literature at a limited scope [1-6]. Furthermore, the impact load scenario or testing procedure can be implemented in a finite element model (FEM) to predict the structural response against impact [10]. The FEM discussed in this study considers small-scale specimens (500 mm in length), which were also experimentally tested in view of validation of the model.

## 2. Experimental Methodology

The experiments were conducted with the help of a drop-weight tower to validate the numerical model. Each concrete beam specimen of size 500 mm x 50 mm x 50 mm was impacted with 6 kg drop-weight at a 1-meter drop-height. Six specimens were tested as indicated in Fig. 1 and Table 1. Considering that each test was conducted 3 times, basically 2 specimen types were tested. Firstly, unstrengthened reinforced concrete reference specimens, designated C1 till C3, and secondly, specimens strengthened with CFRP, designated CFRP1 till CFRP3. The applied drop-weight consists of two parts, the impacting part consist of a spherical steel ball of diameter 62.6 mm which is welded to a steel surcharge with 260 mm length. To control the drop-height an electromagnet system was used. A similar drop-weight tower was previously used by Snoeck et al. [11]. The concrete mix was characterized by the use of ordinary Portland cement combined with a coarse aggregate of size 2/8 mm and a fine aggregate of size 0/5 mm. All specimens were reinforced internally with one steel rebar of 8 mm diameter in the flexural zone by furnishing a concrete cover of 15 mm. The average compressive cube strength was 42 MPa at 28 days (tested on cubes with side length 150 mm) and the nominal tensile strength of the steel rebar was tested 475 MPa. The 50 mm wide and 0.111 mm thick (equivalent dry-fibre thickness) unidirectional carbon fibre sheet was bonded on the soffit of the concrete specimen at a length of 400 mm as shown in Fig 1. The procedure stated in *fib*-Bulletin 90 [9] for the application of FRP was followed to apply CFRP sheet on the concrete. The CFRP sheet has a tensile strength of 3500 N/mm$^2$ and an elastic modulus of 233000 N/mm$^2$ with an ultimate strain of 1.25%. The same CFRP material was also used in the previous study [12]. The wet-layup method was used for the application of the CFRP sheet. The surface of the specimens was grinded and cleaned before the application of a solvent-free 2-component epoxy. The prepared CFRP strengthened specimens were allowed to cure for more than 7 days. To record the high-speed activity of impact load, amongst other three displacement laser sensor were placed beneath the soffit mid-span at three points, shown in Fig 1. A sampling rate of 50 kHz was implemented via the data acquisition system (type NI 6225). The maximum inbound deflections recorded by the laser sensors are given in Table 1. Due to high-frequency recordings, some data was lost due to signal interference, which is denoted by '#' in Table 1.
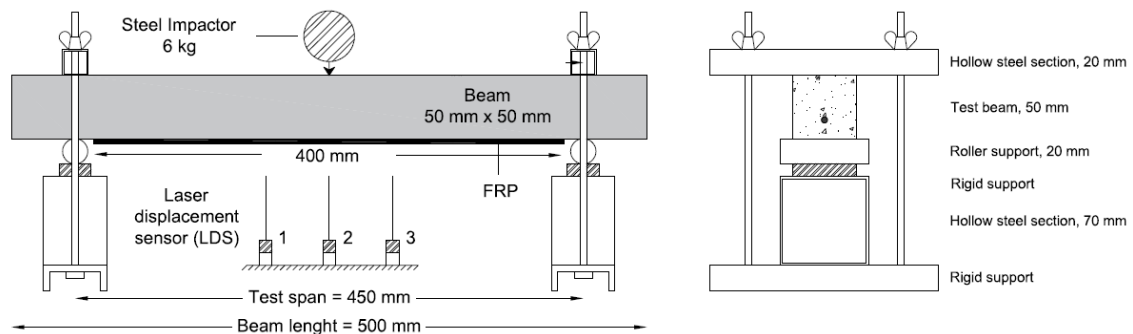


Figure 1. Test setup and instruments used.

Table 1. Displacement recorded by laser sensor during experiments

| Sample Name | CFRP strengthening | Drop-weight (kg) | Drop-height (m) | Maximum displacement (mm) | | | Damage due to impact |
|---|---|---|---|---|---|---|---|
| | | | | Left | Centre | Right | |
| C1 | No | 6 | 1 | -4.6 | -5.9 | -4.7 | Failed |
| C2 | No | 6 | 1 | -4.3 | -5.6 | -4.7 | Failed |
| C3 | No | 6 | 1 | # | # | # | Failed |
| CFRP1 | Yes | 6 | 1 | -1.9 | -2.3 | -2.7 | Not failed |
| CFRP2 | Yes | 6 | 1 | # | # | # | Not failed |
| CFRP3 | Yes | 6 | 1 | -1.7 | -2.2 | -1.7 | Not failed |

# 3. Finite Element Model

The FE simulation is conducted by using the explicit non-linear finite element model program LS-DYNA. 3-dimensional solid modelling was adopted to predict and simulate the behaviour under impact loading. The pre-processing was performed on LS-DYNA version 910 and post-processing using LS-PrePost version 4.5. The concrete beam, steel supports, steel impactor, and FRP strip are designed by automatic shape mesher as given by Figure 2. The model is composed of 3D solid elements, except for the for internal reinforcement which is assigned to behave as a beam element and the FRP strip for which shell elements have been considered. Beam elements are 1-dimensional elements and is suitable to use when the length of the element is much greater than the width or depth. Shell elements are 2-dimensional elements and can be opted if length and width are greater than its thickness.
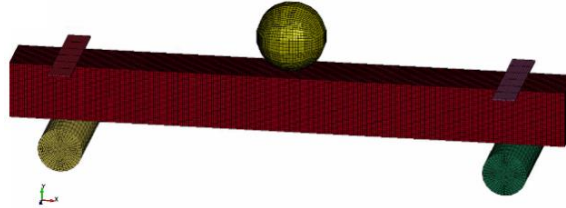


Figure 2. Perspective view of FE model.

## 3.1. Steel material model

The steel material model PLASTIC_KINEMATICS (MAT_003) was used for the steel impactor, steel plate and steel supports. The model is suitable for designing isotropic materials with kinematic hardening plasticity. To create contact between steel impactor and concrete specimen, AUTOMATIC_SURFACE_TO_SURFACE contact model is used. This contact model automatically establishes a connection with external surfaces and checks for collision or penetration. The surcharge of the impactor was considered implicitly, via the weight definition of the ball impactor.

## 3.2. Internal steel reinforcement

The material model PIECEWISE_LINEAR_PLASTICITY (MAT_024) is used to represent the internal reinforcement. The model is suitable for designing of elasto-plastic materials and is commonly used to represent rebars in the form of beam elements. To create a heterogeneous connection between concrete and internal steel reinforcement CONSTRAINT_BEAM_IN_SOLID is used. This interface provides constraint-based coupling of beam elements in solid element.

## 3.3. Concrete material model

In LS-DYNA, there are multiple material models for the representation of concrete and each has a specific constitutive law to respond to the acting load. In this study, the Winfrith (WIN) concrete model (MAT_84) and the Continuous Surface Cap Model (CSCM) concrete model (MAT_159) are used to represent the concrete. The Winfrith model is a basic plasticity model, based on the Ottosen plasticity model, which refers to increased material shearing capacity under hydrostatic pressure (shear surface). Though this model does not considers damage accumulation, it has the capability of crack mapping via an auxiliary post-processing step. The CSCM concrete model which is also known as Schwer and Murry Cap model, is a so-called cap plasticity model with smooth transition between the shear surface and the hardening compaction surface (cap). This model further uses a damage function to consider softening and modulus of elasticity reduction. Although different concrete models can be used, the Winfrith concrete model is often applied for impact load responses [13-15], while the CSCM model can efficiently determine the tensile damage zone by considering the effective plastic strain. An effective plastic strain is an internal damage parameter which characterises the nonlinear damage behaviour and highlights the elements that are actively yielding in the elastic-plastic model (beyond elastic strain and when concrete damage starts to elongate). Both concrete models consider strain rate effects via an incorporated dynamic increase factor (DIF). The Winfrith concrete model uses strain rate enhancement

provided by Broadhouse and Attwood [16], whereas, the CSCM concrete model uses strain rate enhancement by the CEB-FIP Model Code 90 [17]. A general discussion on concrete models in LS-DYNA and comparison of the usage of concrete models under impact loading can be found elsewhere [15, 18].

### 3.4. Carbon fibre reinforced polymer model

In LS-DYNA, there are different predefined material models for FRP and their simulated behaviour is governed by the selection of a material model. The main differences among these material models are the failure criteria and post-damage behaviour. Tested specimens with CFRP strengthening did not collapse, indicating that the CFRP strip remained in the elastic stage. In this regard, the material model used for the CFRP composite is the elastic material model ORTHOTROPIC_ELASTIC (MAT_2). The model is designed to handle orthotropic and isotropic materials with no specific failure criterion [19]. The contact between the concrete and the CFRP strip was considered as a tiebreak element representing the adhesive bond interface. The command (AUTOMATIC_SURFACE_TO_SURFACE_TIEBREAK) allows the modelling of connections transmitting both normal and shear stresses [19]. The failure of contact between the FRP composite and the concrete surface occurs if:

$$\left(\frac{|\sigma_n|}{NFLS}\right)^2 + \left(\frac{|\sigma_s|}{SFLS}\right)^2 \geq 1$$

Where, $\sigma_n$ and $\sigma_s$ are the normal and shear stresses at the interface, respectively. NFLS and SFLS are the normal failure stress and shear failure stress, respectively.

## 4. Results

### 4.1. Displacement

The maximum experimental displacement in vertical direction was measured at three points by the laser sensors. The vertical displacements were compared with the simulated displacement at the corresponding locations, via a built-in fringe component for displacement at the respective node , as mentioned in Table 2 and Table 3. The mid-span displacements recorded experimentally and numerically for the specimens with and without CFRP are plotted in Fig 3. Fig 3 indicates a good correspondence of the inbound stage, and corresponding value of the maximum inbound deflection, especially for the CFRP strengthened specimens. In terms of rebound stage, experimental values reached somewhat unexpected larger upwards deflections and in some cases even a small upward residual deflection. This behaviour was not confirmed by the simulation. This discrepancy is attributed to the detailing of the set-up fixation, which might have been less rigid as anticipated and resulted in settlements of the set-up during rebound, not encountered for by the laser sensors. Mainly for the unstrengthened reference specimens, it is further noted that the stiffness response (as can be observed from the period of the oscillation) is not fully captured by the simulation. This might be attributed to the boundary conditions at the supports, meaning the degree of clamping. More simulations with respect to the sensitivity to the boundary conditions are needed in this respect. On overall, the FEM yielded promising results and will form the basis for further experimental and numerical work.

The comparison of experimental and numerical results in terms of maximum midspan inbound deflection is also illustrated in Fig 4. The numerical prediction of maximum displacement if compared with experimental results corresponds 100% for the WIN concrete model and 120% for the CSCM model, in the case of the strengthened specimens. However, the unstrengthened specimens showed a correspondence of 140% for the WIN concrete model and 67% for the CSCM concrete model. Comparing the maximum deflection of the strengthened specimen versus the unstrengthened specimen, the application of CFRP enhanced the impact resistance of the concrete by reducing the maximum displacement at the centre point by 60%. The simulation exhibited similar behaviour and showed a reduced maximum displacement at the centre point of 74% and 50% for the CSCM concrete model and the WIN concrete model, respectively.
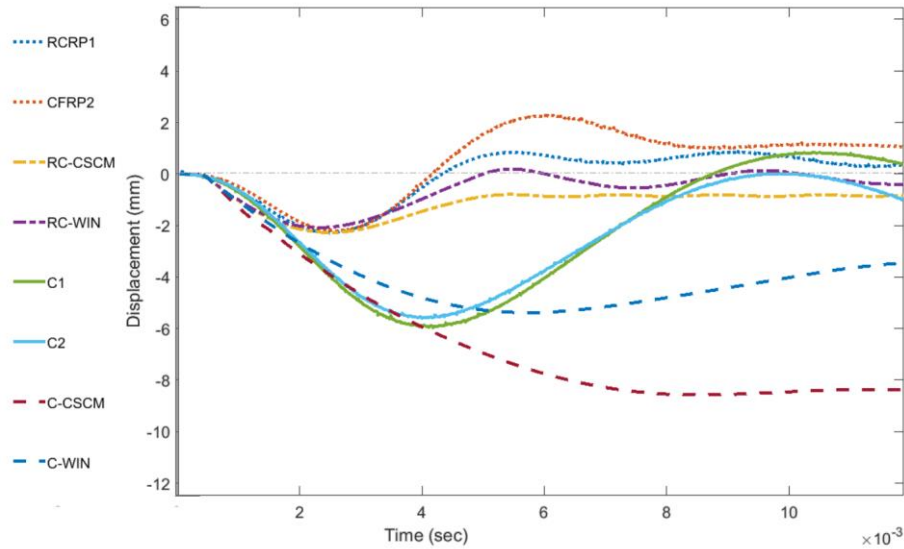
Figure 3. Experimental and FEM displacement values at mid-span of concrete beam.

Table 2. Displacement on centre point

| Sample | CFRP | Displacement | | Experimental / FEM |
|---|---|---|---|---|
| | | FEM (centre) | Exp. (centre) | |
| C-CSCM | No | -8.5 | -5.9 | 0.69, 0.65 |
| C-WIN | No | -4.0 | -5.6 | 1.4, 1.4 |
| CFRP-CSCM | Yes | -2.2 | -2.3 | 1.0, 1.0 |
| CFRP-WIN | Yes | -2.0 | -2.2 | 1.15, 1.1 |

Table 3. Displacement on right point

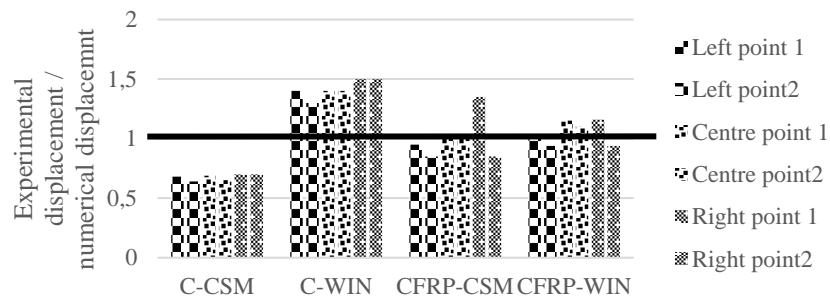| Sample | CFRP | Max. Displacement | | Experimental / FEM |
|---|---|---|---|---|
| | | FEM (right) | Exp. (right) | |
| C-CSCM | No | -6.7 | -4.7, -4.7 | 0.7, 0.7 |
| C-WIN | No | -3.1 | | 1.5, 1.5 |
| CFRP-CSCM | Yes | -2.0 | -2.1, -1.7 | 1.35, 0.85 |
| CFRP-WIN | Yes | -1.8 | | 1.16, 0.94 |



Figure 4. Ratio of experimental and predicted FEM displacement values.

## 4.2. Failure aspect

The failure aspect has been assessed on via the CSCM based simulation, by considering the effective plastic strain. In the actual experiment, all unstrengthened specimens failed by critical flexural cracking at mid-span. For the CFRP strengthened specimens no critical mid-span cracking was observed and specimens did not fail.

For the unstrengthened reference specimen the numerical failure aspect at mid-span (Fig. 5) was in line with the experimental behaviour. The numerically observed top cracking near the supports deviated from the experimental observations, and might indicate that the boundary conditions at the support zone are not yet fully captured by the simulation.

For the strengthened specimen, which did not fail, the numerical model (Fig. 6) predicted initiation of shear cracks at the ends of the CFRP, though this was not observed experimentally. At the other hand a midspan flexural crack was observed experimentally at the top of the specimen, likely due to the rebound deformations and possibly further influenced by the impactor which rebounded and hit the specimen once more. It should be noted that the simulation only considers one impact. To examine the crack development of the concrete under impact load, the use of high-speed camera is highly recommended for future studies.
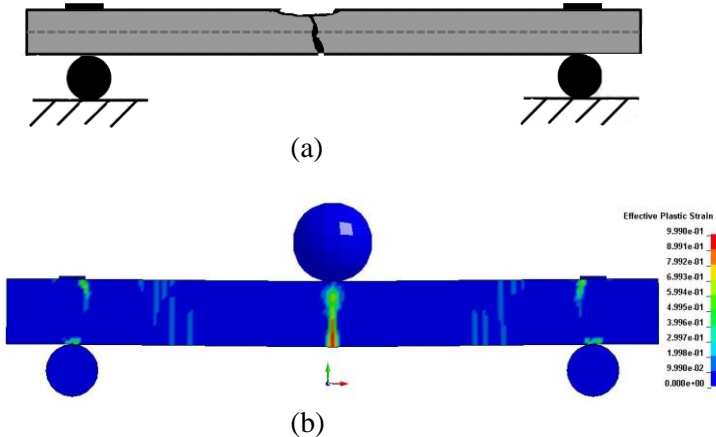


(a)



(b)

Figure 5. Crack pattern of concrete beam specimens without CFRP strengthening (a) Experimental (b) FEM.
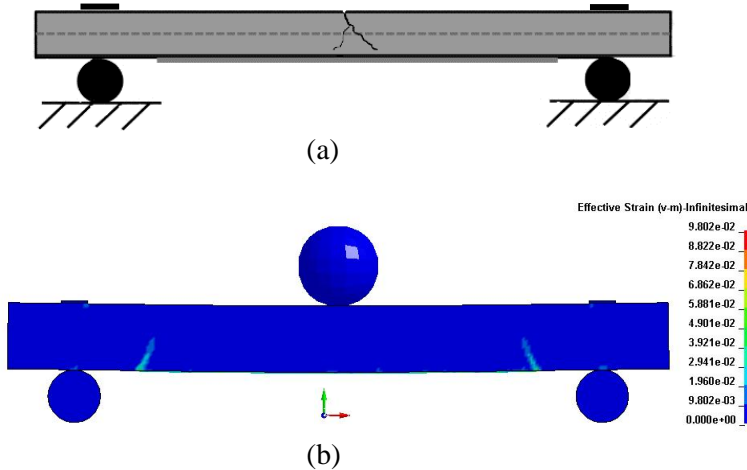


(a)



(b)

Figure 6. Crack pattern of concrete beam specimens with CFRP strengthening (a) Experimental (b) FEM.

## 5. Conclusions

It can be concluded based on the experimental observations that the CFRP strengthening enhances the impact resistance of the reinforced concrete under impact load. The application of CFRP on the specimens significantly reduced the maximum inbound displacement at mid-span by 60%, and arrested the occurrence of a critical flexural crack. These experimental observations were validated using a numerical simulation. The FE simulation using the CSCM concrete model demonstrated 74% reduction in the displacement on the application of CFRP strengthening on concrete beam specimens, whereas,

the WIN concrete model indicated a 50% reduction. The promising results obtained in this preliminary study demonstrate the suitability and potential of the numerical approach to study and predict the impact response of reinforced concrete members strengthened with CFRP.

# 6. References

1. Weizhang Laio, M. Li, W. Zhan and Z. Tian. (2017). Experimental studies and Numerical Simulation of behaviour of RC beams retrofitted with HSSWM-HPM under impact loading. *Engineering Structures,* 149(131-146).
2. Kurihasi, Y., H. Kon-ho, H. Mikami and N. Kishi. (2015). *Falling-weight impact test of Flexural Strengthened RC beams with AFRP sheet*. In: Responce of Structures under Extreme Loading (PROTECT 2015).
3. Pham, T. and H. Hao. (2016). *Confinement efficiency of concrete cylinders wrapped with different types of FRP under impact loads*. In: 24th Australasian Conference on the Mechanics of Structures and Materials, Perth, Australia.
4. Tang, T. and H. Saadatmanesh. (2003). Behavior of Concrete Beams Strengthened with Fiber-Reinforced Polymer Laminates under Impact Loading. *Journal of composites for construction,* 3, 209-218.
5. Thong M. Pham and H. Hao. (2016). Impact Behavior of FRP-Strengthened RC Beams without Stirrups. *Journal of Composites for Construction,* 20(4).
6. M. A. Erki, U.M. (1999). Impact Loading of Concrete Beams Externally Strengthened with CFRP Laminates. *Journal of Compostie for Constructions,* 3(3), 117-124.
7. Jaganathan, J., E. Pournasiri, K.K. Choong, C.G. Tan, and F. De'nan. (2011). External CFRP repairing of pretested beams reinforced using pre-stress rebars. *Journal of Reinforced Plastics and Composites,* 30(20), 1753-1768.
8. ACI 440.2 R-17: Guide for the Design and Construction of Externally Bonded FRP Systems for Strengthening Concrete Structures.
9. fib Bulletin 90: Externally bonded FRP reinforcement for RC structures. 2019.
10. Maazoun, A., Bachir Belkassem, Bruno Reymen, Stijn Matthys, John Vantomme, and David Lecompte. (2018). Blast Response of RC Slabs with Externally Bonded Reinforcement: Experimental and Analytical Verification. *Composite Structures,* 200(246-257).
11. Snoeck, D., T.D. Schryver and N.D. Belie. (2018). Enhanced impact energy absorption in self-healing strain-hardening cementitious materials with superabsorbent polymers. *Construction and Building Materials,* 191, 13-22.
12. Matthys, S. (2000). *Structural Behaviour and Design of Concrete Members Strengthened with Externally Bonded FRP Reinforcement.* (PhD thesis), Ghent University., Ghent, Belgium.
13. Broadhouse, B.J. and A.J. Neilson. (1987). *Modeling reinforced concrete structures in DYNA3D*
14. Algaard, W., J. Lyle and C. Izatt. (2005). *Perforation of composite floors*. In: 5th European LS-DYNA users conference, Brimingham, UK.
15. Memon, D., A. Maazon, S. Matthys and D. Lecompte. (2019). *Low-velocity impact behaviour of plain concrete beam*. In: 12th LS-DYNA European conference and users meeting, Koblenz, Germany.
16. Broadhouse, B.J. and G.J. Attwood. (1993). *Finite Element Analysis of the Impact Response of Reinforced Concrete Structures using DYNA3D*. In: Proceedings of Structural Mechanics in Reactor Technology (SMiRT) 12, University of Stuttgart Germany
17. CEB-FIP Model Code: Design Code 1990.
18. Youcai, W., J.E. Crawford and J.M. Magallanes. (2012). *Performance of LS-DYNA concrete constitutive models*. In: 12th International LS-DYNA Users Conference.
19. LSTC. (2016). *LS-Dyna Keyword user's manual* (Vol. 1).